### Title

PARP Inhibition Enhances Radiotherapy of SMAD4-Deficient Human Head and Neck Squamous Cell Carcinomas in Experimental Models




### Journal

Clinical Cancer Research, 26(12)

### ISSN

1078-0432



### Authors

Hernandez, Ariel L
Young, Christian D
Bian, Li
et al.



### Publication Date

2020-06-15

### DOI

10.1158/1078-0432.ccr-19-0514

Peer reviewed

HHS Public Access

Author manuscript

*Clin Cancer Res*. Author manuscript; available in PMC 2020 December 15.

Published in final edited form as:

*Clin Cancer Res*. 2020 June 15; 26(12): 3058–3070. doi:10.1158/1078-0432.CCR-19-0514.

# PARP inhibition enhances radiotherapy of SMAD4 deficient human head and neck squamous cell carcinomas in experimental models

**Ariel L. Hernandez**[1,*], **Christian D. Young**[1,*], **Li Bian**[1], **Kelsey Weigel**[1], **Kyle Nolan**[1], **Barbara Frederick**[2,**], **Gangwen Han**[1,***], **Guanting He**[1], **G. Devon Trahan**[3], **Michael C. Rudolph**[4], **Kenneth L. Jones**[3], **Ayman J. Oweida**[5], **Sana D. Karam**[2], **David Raben**[2], **Xiao-Jing Wang**[1,6,****]

[1]Department of Pathology, School of Medicine, University of Colorado, Anschutz Medical Campus, Aurora, CO

[2]Department of Radiation Oncology, University of Colorado, Anschutz Medical Campus, Aurora, CO

[3]Department of Pediatrics, Section of Hematology, Oncology, and Bone Marrow Transplant, University of Colorado, Anschutz Medical Campus, Aurora, CO

[4]Department of Medicine, division of Endocrinology, Metabolism, and Diabetes. University of Colorado, Anschutz Medical Campus, Aurora, CO

[5]Department of Nuclear Medicine and Radiobiology. Université de Sherbrooke, Sherbrooke, Quebec

[6]Veterans Affairs Medical Center, VA Eastern Colorado Health Care System, Aurora, CO

## Abstract

**Purpose—***SMAD4* loss causes genomic instability and the initiation/progression of head and neck squamous cell carcinoma (HNSCC). Here, we study if SMAD4 loss sensitizes HNSCCs to olaparib (PARP inhibitor) in combination with radiotherapy (RT).

**Experimental Design—**We analyzed HNSCC TCGA data for *SMAD4* expression in association with FAN*C/BRCA* family gene expression. Human HNSCC cell lines were screened for sensitivity to olaparib. Isogenic HNSCC cell lines were generated to restore or reduce SMAD4 expression and treated with olaparib, radiation, or the combination. HNSCC pretreatment specimens from a Phase I trial investigating olaparib were analyzed.

**** Corresponding Author: Xiao-Jing Wang MD, PhD, University of Colorado School of Medicine, 12800 East 19th Avenue, Mail stop 8104, Aurora, CO 80045, Phone: (303) 724-3001, Fax: (303) 724-4730, xj.wang@cuanschutz.edu.

** Current address: Department of Molecular, Cellular and Developmental Biology, University of Colorado Boulder, CO

*** Current address: Department of Dermatology, Peking University International Hospital, China

* The authors contributed equally to this publication

Author contributions

ALH, XJW, DR, and CDY designed experiments. SDK and AJO advised on experimental designs and data presentation. ALH, CDY, KN, KW performed *in vivo* and *in vitro* experiments. BF performed olaparib IC50 assay in cell lines. LB, GTH, GWH performed immunostaining and analyses. KLJ, MCR, GDT performed bioinformatics analyses. ALH, CDY, and XJW analyzed data and wrote the manuscript. All authors provided input into manuscript writing and editing.

**Conflict of interest:** The authors declare no potential conflicts of interest.

**Results—***SMAD4* levels correlated with levels of *FANC/BRCA* genes in HNSCC. HNSCC cell lines with *SMAD4* homozygous deletion were sensitive to olaparib. *In vivo*, olaparib or RT monotherapy reduced tumor volumes in *SMAD4* mutant but not *SMAD4* positive tumors. Olaparib with RT dual therapy sustained tumor volume reduction in *SMAD4* deficient (mutant or knockdown) xenografts, which exhibited increased DNA damage and cell death compared to vehicle treated tumors. *In vitro*, olaparib alone or in combination with radiation caused lower clonogenic survival, more DNA damage-associated cell death and less proliferation in *SMAD4* deficient cells than in *SMAD4*-positive (endogenous SMAD4 or transduced SMAD4) cells. Applicable to clinic, 5 out of 6 SMAD4-negative HNSCCs and 4 out of 8 SMAD4-positive HNSCCs responded to a standard treatment plus olaparib in a Phase I clinical trial, and SMAD4 protein levels inversely correlated with DNA damage.

**Conclusion—***SMAD4* levels are causal in determining sensitivity to PARP inhibition in combination with RT in HNSCCs.

## Introduction

Worldwide, head and neck cancer is the sixth most common cancer type (1); over 90% are HNSCC (2). Among HNSCCs, human papilloma virus (HPV) and tobacco consumption are the two major etiologies (3). Tobacco-associated HNSCCs have worse outcomes than HPV-associated HNSCCs. Despite recent advances in therapeutic approaches, HNSCC patients have a 5-year survival rate of 40 – 50% (3,4).

In tobacco associated HNSCCs, increased DNA repair rescues tumor cells from dying of DNA damage-associated cell death, contributing to treatment failure (3,5). Among DNA repair molecules, the *FANC/BRCA* family genes are uniquely associated with HNSCC susceptibility, i.e., Fanconi Anemia survivors (with germline *FANC/BRCA* gene mutations) have a high susceptibility to HNSCC (6). The US Food and Drug Administration (FDA) has approved several Poly-ADP ribose polymerase (PARP) inhibitors to treat advanced ovarian and metastatic breast cancers with *BRCA* mutations because blockade of PARP-mediated DNA repair is synthetically lethal in the context of mutant *BRCA1/BRCA2* inducing DNA damage-associated death in cancer cells. Loss of *BRCA1 and BRCA2,* primarily through loss-of-functional mutations, occur in 2.2% and 5% human HNSCCs, respectively (7). Therefore, alternative molecular markers are needed to predict therapeutic response of PARP inhibitors. Among such potential molecular markers, *SMAD4* loss represents a promising candidate. 35 – 52% of human HNSCCs lose at least one copy of *SMAD4* gene, largely through chromosomal deletion, and the remaining allele can be lost through homozygous deletion, loss of heterozygosity, and transcriptional silencing (8,9). Further, HNSCCs with heterozygous *SMAD4* deletion contain homozygous *SMAD4* deleted cells in their heterogeneous cell populations (9).

SMAD4, a tumor suppressor in the TGFβ signaling pathway, regulates proliferation, apoptosis, and genomic stability (10,11). Loss of *SMAD4* is detected in early stage human HNSCCs and *Smad4* deletion in mice causes spontaneous HNSCCs (11). We have shown that *Smad4* null HNSCCs have genomic instability associated with decreased *Brca1* and *Rad51* expression (abnormal centrosome numbers, high mutational load and hypersensitivity

to mitomycin-C induced chromosomal crosslinking and breakage), and in human HNSCC tissue arrays, SMAD4 levels correlate with BRCA1 and RAD51 levels (11). Further, expression of several *FANC/BRCA* genes is reduced by knocking down SMAD4 in human keratinocytes but reinstated by SMAD4 restoration in HNSCC cells; and BRCA/RAD51 DNA repair foci are reduced in *SMAD4* mutant HNSCC cells but restored with *SMAD4* expression (11). These findings suggest *SMAD4* loss plays a causal role in downregulation and functional defects of FANC/BRCA genes in HNSCCs, resulting in a "*BRCA*-like" phenotype (12). The remaining questions we sought to answer are: 1. whether SMAD4 deficient "BRCA-like" molecular signatures apply to HNSCC patients and 2. whether the SMAD4 deficient "BRCA-like" phenotype is sufficient to impact therapeutic interventions. Because other cancer types with a "BRCA-like" phenotype, i.e., decreased expression and function of *FANC/BRCA* family gene(s) necessary for DNA repair (13), have shown susceptibility to PARP inhibitors like olaparib (14–16), we sought to explore if *SMAD4* mutant HNSCCs are susceptible to PARP inhibition. Clinical trials have shown olaparib is well tolerated by HNSCC patients (17). Given that RT is a standard of care for locally advanced HNSCCs, we tested olaparib in combination with RT in HNSCCs with or without *SMAD4* deficiency and analyzed cellular mechanisms by which *SMAD4* loss contributes to the therapeutic response.

## Methods and Materials

### Analysis of TCGA Data

The human HNSCC provisional sequencing data set was queried for mRNA expression z-scores for *SMAD4* and *FANC/BRCA* family genes *via* cBioPortal for Cancer Genomics (18,19) Among 530 HNSCC cases, 522 had genotype/expression information, 116 cases were tested for HPV, and 42 were HPV+ (TCGA, Provisional, queried: 8/29/2019). Because HPV status is not known for all samples, we included all cases for analyses.

### Human HNSCC Cell Lines Clonogenic Assays

Human HNSCC cell lines were collected under Materials and Transfer Agreements (MTAs), and authenticated by the Tissue Culture Shared Resource at the University of Colorado Cancer Center and tested for mycoplasma every 3 months. 200–3,200 cells were seeded to six or twelve well plates, treated with 0, 0.1, 1 or 5 μM olaparib and 0–6 Gy RT and cultured for 8–14 days for clonogenic assay using criteria as previously described (20). Fresh media containing drugs was applied every three days. Colonies were fixed and stained with 1% crystal violet in methanol. Colonies containing 50 or more cells were counted, plotted on log scale graphs and fitted using the linear-quadratic model (21). There were 3 – 6 replicates for each treatment.

### Generating Isogenic HNSCC Cell Lines

CAL27, a human tongue *SMAD4* mutant tumor cell line (22), was purchased from ATCC (#CRL-2095). To conditionally express *SMAD4*, pLenti-CMV-rtTA3-blast vector (Addgene, #26429-LV) was transduced into CAL27 cells. After blasticidin selection, pLVX-tight-Puro FLAG-SMAD4 TetON (+SMAD4) or FLAG-empty TetON (+empty vector) construct (provided by the Massague lab (23)) was transduced by lentivirus into CAL27-rtTA3 cells

and selected with puromycin. UMSCC1, a floor-of-the-mouth derived tumor cell line was provided by the Carey lab (24) and validated by fingerprint sequencing. *SMAD4* shRNA (*shSMAD4*) or non-targeting control shRNA (*shCTRL*) (sequences in Supplementary Table 1) was inserted into a tet-pLKO-neo vector (Addgene, #21916) and transduced by lentivirus into UMSCC1 cells, then selected with G418. Doxycycline concentration was optimized for induction of *SMAD4* expression in CAL27-rtTA3 cells or to knockdown *SMAD4* in UMSCC1 cells. HaCaT keratinocytes were purchased (Addexbio, #T0020001).

## qRT-PCR and Western Blotting

RNA Plus mini Kit (Qiagen, #74136) was used to extract total RNA from cells. Relative *SMAD4, KRT14,* or *FANC* family genes was determined with TaqMan assays using Brilliant II QRT-PCR 1-step Master Mix kit (Agilent, #600809) for each reaction. Ct values of the gene of interest and *KRT14* were used to determine relative fold change by $2^{-\Delta\Delta Ct}$. Proteins were harvested with RIPA buffer (Cell Signaling, #9806S) supplemented with protease and phosphatase inhibitor cocktails (Roche, #5892970001 and #4906845001). Western blotting was performed using standard protocols and detected using an Odyssey imager. Antibodies and TaqMan assays are described in Supplementary Table 1.

## Animal Studies

Animal studies were approved by the University of Colorado AMC IACUC. Athymic female, 6–8-week-old nude mice were purchased from Jackson Laboratories. Cells ($1 \times 10^6$) were suspended in 50% Matrigel (ThermoFisher, #CB-40234) and injected subcutaneously into the flanks of mice. When tumors reached 100 $mm^3$, doxycycline (2 g/L) was administered in sugar water (4 g/L) and maintained throughout the study. At 300 – 400 $mm^3$, the mice were randomized into treatment groups at day 0. At day 1, mice received olaparib (25 mg/kg, gavage) or vehicle, and beginning on day 3, tumors were directly exposed to fractionated RT every 3 days (3 Gy x 6 = 18 Gy). Olaparib was formulated in 10% v/v DMSO / 50% v/v of 30% w/v kleptose. An RS2000 instrument was used for x-ray irradiation of cells and animals. Vehicle or olaparib treatments continued through the entire study and tumor burden (weight loss, tumor size, etc.) was monitored to determine study end. Tumor volume was determined by the formula, volume = (width x width x length)/2. Tumors were collected for molecular and morphological analysis after sacrifice.

## TUNEL Assay, Immunofluorescence and Immunocytochemistry

Apoptotic cells were stained using a commercially available Fluorometric TUNEL kit (Promega, #G3250) per the provided protocol. Immunofluorescence staining was performed on xenograft tumor specimens collected at the end of each study and immunocytochemistry was conducted for cellular kinetics. Primary antibodies used are detailed in Supplementary Table 1. Samples were counterstained with DAPI and Alexa Fluor-conjugated secondary antibodies (ThermoFisher) were used for detection. For xenograft or primary HNSCCs, 3–5 immunofluorescence regions were averaged for quantification of TUNEL+, pH2AX+, or Ki67+ cells per specimen; 3–7 tumors per group were used for analyses. For pH2AX immunocytochemistry, plates were fixed at 0, 1, 8, 24, and 48 hours post-radiation using 10% neutral-buffered formalin. For Ki67 staining, plates were fixed at 0 and 48 hr. Plates were stored in PBS with 0.02% $NaN_3$ at 4°C until all time points were collected and

molecularly labeled as described above. Stained 96 well plates were imaged using an Opera Phenix Imaging System with Harmony software (High-throughput Screening Core, University of Colorado) to determine the number of pH2AX foci per nucleus or the number of Ki67-positive cells over time.

### Analysis of pretreatment HNSCC specimens in Phase I trial of olaparib plus RT and cetuximab

Locally advanced HNSCC patients were enrolled in a Phase I trial and treated with olaparib with concurrent radiation and cetuximab (see details in enrollment criteria and treatment regimens in original report) (17). Pretreatment biopsies were collected under the IRB approval and used to perform SMAD4 fluorescence in situ hybridization (FISH) as previously reported (9), SMAD4 immunostaining was performed as described above and scored for tumor epithelial intensity between 0 (no staining) and 3 (equivalent to normal epithelial staining). Immunofluorescence of pH2AX was performed as described above and scored between 1 (<20% foci-positive cells) and 3 (>50% foci-positive cells). The correlation between SMAD4 immunostaining scores and pH2AX scores were analyzed by Pearson's analysis.

## Results

### *SMAD4* Expression Correlated with *FANC/BRCA* Gene Expression Levels in HNSCC Patient Specimens and Olaparib Sensitivity

To determine if "*BRCA*-like" molecular signatures found in mouse HNSCCs and human HNSCC cells (11) apply to a large population of HNSCCs, we analyzed *SMAD4* and *FANC/BRCA* expression levels in TCGA data (18,19). *SMAD4* mRNA expression levels in HNSCCs are generally lower than in normal epithelia (11) and HNSCCs with *SMAD4* downregulation are expected to have <50% of normal *SMAD4* mRNA levels; therefore, our criteria for *SMAD4* downregulation was <−1.5 standard deviations from the mean and *SMAD4* upregulation >1.5 standard deviations from the mean. Among all 530 HNSCC cases, 42/116 tested cases were $HPV^{+}$. *SMAD4* was down-regulated in 17% (n = 88; "$SMAD4^{low}$") and up-regulated in 7% (n = 38; "$SMAD4^{high}$") of human HNSCCs. Strikingly, $SMAD4^{low}$ patients appeared to have decreased expression of many *FANC/BRCA* family genes; conversely, $SMAD4^{high}$ HNSCCs had increased expression of *FANC/BRCA* family genes (Figure 1a). Intriguingly, expression of all 18 *FANC/BRACA* genes was lower or unchanged in $SMAD4^{low}$ cases compared to all other cases, and none was higher (Supplementary Figure S1a). Analysis of all HNSCC cases revealed a positive correlation (and no negative correlations) between *SMAD4* and each of the 18 *FANC/BRCA* genes (Supplementary Figure S1b), although some correlations were weak, suggesting other regulatory pathways for these genes. Overall, there were more HNSCC cases with decreased expression of one or more *FANC/BRCA* family genes in $SMAD4^{low}$ HNSCCs compared to $SMAD4^{high}$ HNSCCs (Figure 1b). Because previous studies have shown "BRCA-like" molecular changes in other cancer types outside of the *Fanc/Brca* family (25–27), we performed a gene set enrichment analysis (GSEA) against the 50 hallmark genes using the expression data of $SMAD4^{low}$ and $SMAD4^{high}$ samples. Genes in the "DNA repair" hallmark gene set trended toward enrichment in these *SMAD4* down- or up-regulated

HNSCCs (Figure 1c) but not as strongly as the enrichment observed in Fanconi Anemia pathway gene set (Supplemental Figure S2). To assess if *SMAD4* genetic loss correlates with the olaparib sensitivity seen in *BRCA* mutant tumors, we performed a clonogenic survival assay in a panel of human HNSCC cell lines in response to olaparib treatment (0, 0.5, 1, and 5 μM). Cell lines insensitive to olaparib were without *SMAD4* loss, and cell lines with *SMAD4* loss were sensitive to olaparib (Figure 1d–e). Two *SMAD4* wildtype cell lines were sensitive to olaparib independent of *SMAD4* loss.

## Higher Sensitivity of *SMAD4*-Deficient HNSCC Xenografts to Dual Olaparib/RT Treatment than SMAD4-Positive HNSCC Xenografts *In Vivo*

To assess if *SMAD4* loss plays a causal role in HNSCC sensitivity to DNA damaging therapeutic agents, we generated isogenic cell lines from *SMAD4* mutant (CAL27) and *SMAD4* wildtype (UMSCC1) HNSCC lines by restoration of *SMAD4* in CAL27 and knockdown of *SMAD4* expression in UMSCC1 cells using doxycycline-inducible systems. These cell lines modulated SMAD4 protein and transcript expression in response to doxycycline treatment as expected (Supplementary Figure S3a–c). Additionally, expression of *SMAD4* in CAL27 induced the relative expression of all nine of the *FANC* family genes examined and *SMAD4* knockdown in UMSCC1 reduced the relative expression of 6/9 *FANC* family genes (Supplementary Figure 3d). We then tested the influence of SMAD4 on therapeutic responses in xenograft tumors (Figure 2a). CAL27+empty vector (*SMAD4* mutant) xenografted tumors had a long latency prior to olaparib response, i.e., ~5 weeks before tumor volumes declined, with long-term responses apparent in three out of five tumors (Figure 2b). RT alone rapidly reduced tumor volume; however, tumors began to grow after five weeks (Figure 2b). Dual olaparib and RT treatment reduced all tumor volumes to the baseline (Figure 2b, 2e).

To determine if *SMAD4* restoration in CAL27 tumors would attenuate the therapeutic effects observed with *SMAD4* loss, we transplanted CAL27+*SMAD4* cells prior to doxycycline-induction. Once tumors were >300 $mm^3$, doxycycline was administered to induce SMAD4 expression in CAL27 tumors. However, doxycycline-induced *SMAD4* expressing tumor xenografts failed to enter growth phase even when we transplanted 10x more CAL27+*SMAD4* cells (Supplementary Figure S4). When doxycycline induction of *SMAD4* expression was discontinued, these tumors rapidly entered growth phase, confirming that *SMAD4* restoration was the cause of blunted tumor growth. Although this result prevented assessment of therapeutic effects in these tumors, it verified that *SMAD4* is a strong tumor suppressor in HNSCC.

In complement, we tested therapies in SMAD4-positive UMSCC1 (*shCTRL*) and SMAD4 knockdown (*shSMAD4*) tumors. UMSCC1+*shCTRL* xenograft tumors did not respond to olaparib (Figure 2c, 2f). RT or RT plus olaparib modestly reduced tumor growth, but there was no significant difference between these two treatments (Figure 2c, 2f). Unlike CAL27 tumors, olaparib did not alter UMSCC1+*shSMAD4* xenograft tumor volumes (Figure 2d, 2g). RT transiently reduced UMSCC1+*shSMAD4* xenograft tumor volumes. However, only dual olaparib and RT treatment was sufficient to maintain tumor reduction in UMSCC1+*shSMAD4* xenograft tumors compared to vehicle or RT alone (Figure 2d, 2g).

Finally, we analyzed the number of mice with CAL27 tumors less than 1,200 $mm^3$ or UMSCC1 tumors less than 1,500 $mm^3$ over time and found that RT or olaparib + RT prevented all CAL27 xenografts from reaching 1,200 $mm^3$, significantly different from other treatments (Figure 2h), whereas the olaparib treatment group had two outgrowing, resistant tumors (Figure 2b, 2h). However, only olaparib + RT prevented all UMSCC1+*shSMAD4* tumors from reaching 1,500 $mm^3$, significantly different from RT alone (Figure 2j) while no treatment group significantly influenced UMSCC1+*shCTRL* tumors outgrowth (Figure 2i). These data suggest that *SMAD4* deficient HNSCCs are more prone to respond to olaparib with RT.

## *SMAD4* Deficient HNSCCs Harbor Sustained DNA Damage and Treatment-Associated Apoptosis *In Vivo*

We examined if the reduction in tumor volumes by olaparib/RT dual therapy is due to cell death or decreased proliferation among treatment groups in *SMAD4* deficient xenograft tumors harvested at the final time point of the study. There was a significant increase in apoptotic, $TUNEL^+$ cells with all three treatments in CAL27 (*SMAD4* mutant) and UMSCC1+*shSMAD4* xenograft tumors compared to vehicle-treated tumors (Figure 3a, 3b, 3e, 3f). Dual therapy induced more apoptosis than RT alone or olaparib alone in UMSCC1+*shSMAD4* tumors (Figure 3f). To determine if sustained DNA damage contributed to apoptosis in CAL27 xenograft tumors responding to treatments, we stained tumors with pH2AX and measured the percentage of cells positive for pH2AX foci (>3 foci/nucleus). Significant DNA damage was present in CAL27 xenograft tumors with all three treatments (Figure 3a, 3c). In UMSCC1+*shSMAD4* xenograft tumors, pH2AX+ cells were variable and significantly increased by olaparib or dual treatment (Figure 3e, 3g). However, Ki67 staining to detect proliferating cells showed a moderate increase in RT-treated CAL27 tumors, consistent with their tendency to recover at this late stage but not in tumors treated with olaparib or RT+olaparib (Figure 3a, 3d). Ki67+ cells were more abundant in UMSCC1+*shSMAD4* xenograft tumors than CAL27 tumors, but showed no significant changes among treatment groups (Figure 3e, 3h).

## *SMAD4*-Deficient HNSCC Cells Had Reduced Clonogenic Survival and short term proliferation in Response to Combined Olaparib and Radiation Treatment *In Vitro*

Because the DNA damage-associated cell death found within endpoint tumors could not determine if olaparib + RT treatment induced more apoptosis early in treatment that led to the most effective tumor regression, we examined treatment response *in vitro* with multiple doses of olaparib (0–5 μM) and/or radiation (0–6 Gy) using the same isogenic cell lines in clonogenic colony formation assays. Independent of radiation, olaparib dose-dependently decreased survival of CAL27 lacking *SMAD4* and UMSCC1 with *SMAD4* knockdown compared to their respective control cell lines (Figure 4a, 4b). Similarly, independent of olaparib, the two cell lines with no/low SMAD4 had fewer colonies than their SMAD4-expressing control cell lines in response to 2 or 4 Gy RT (Figure 4c, 4d). CAL27+*SMAD4* cells had reduced sensitivity to 6 Gy RT in combination with all doses of olaparib and lower doses of olaparib in combination with 4 Gy RT compared to CAL27 with mutant *SMAD4* (Figure 4c). UMSCC1+*shSMAD4* were more sensitive than control cells to the combination of all doses of RT and olaparib tested (Figure 4d). To determine if proliferation contributes

to cell survival after combination therapy, we examined Ki67 staining before and after 48 hr radiation in combination with continuous olaparib (1 μM, 10 μM). Ki67-marked proliferation in both *SMAD4* deficient/low cell lines decreased more than their isogenic *SMAD4* positive cell lines in response to radiation or the combination of RT and olaparib (Figure 4e, f); normalization to DMSO to remove the influence of SMAD4 status on baseline RT sensitivity demonstrated that cells with low/no SMAD4 were still more sensitive to the combination of RT and olaparib (Supplementary Figure S5a,b). SMAD4 manipulation, on its own, did not affect short term proliferation (Supplementary Figure S5c,d).

## Olaparib in Combination with Radiation Had Immediate Effects on Enhancing DNA Damage and Apoptosis in *SMAD4*-Deficient HNSCC Cells *In Vitro*

To assess if the extent of DNA damage contributes to reduced cell viability in a *SMAD4* dependent manner, we irradiated cells with or without continuous olaparib exposure, and examined the number of pH2AX foci/cell over 48 hours. All cell lines had increased pH2AX foci by 1 hour after radiation (Figure 5c–d). In CAL27+empty vector cells, pH2AX foci were sustained for 48 after radiation with olaparib whereas pH2AX foci attenuated in CAL27+*SMAD4* cells after 24 hr (Figure 5a, 5c). Similar results were observed in UMSCC1 cells: *SMAD4* knockdown cells demonstrated prolonged pH2AX foci compared to control cells 48 hr post-RT with continuous olaparib (Figure 5b, 5d). Importantly, irradiated *SMAD4*-deficient cells had greater levels of pH2AX foci than *SMAD4*-expressing cells at 48 hr when treated with olaparib (Figure 5c, 5d). Similarly, DNA damage visualized by comet assay revealed that both CAL27 and UMSCC1 with no/low SMAD4 had more DNA damage than their isogenic control cells in response to RT or RT plus olaparib (Supplementary Figure S6).

To determine if accumulated DNA damage is sufficient to trigger apoptosis, we performed western blot analysis for PARP cleavage (cPARP) using our isogenic cells treated +/− 8 Gy and +/− 10 μM olaparib. Full length PARP protein was not changed in any cell line in response to any treatment (Figure 5e, 5f). In CAL27+empty vector cells, cPARP was detectable in response to either olaparib or radiation, and cPARP was more prominent in cells with dual olaparib and radiation treatment (Figure 5e). Strikingly, treatment-induced cPARP was attenuated by *SMAD4* restoration in CAL27 (Figure 5e). In UMSCC1+*shCTRL* cells, cPARP was detectable after radiation but not olaparib treatment, and became prominent in response to olaparib in combination with radiation (Figure 5f). In UMSCC1+*shSMAD4* cells, cPARP became detectable after olaparib treatment, and was more prominent after radiation or olaparib in combination with radiation (Figure 5f). These results confirmed that radiation-induced apoptosis was more potent than olaparib alone and olaparib plus radiation increased apoptosis compared to single treatments and that SMAD4-deficiency increased sensitivity to olaparib + RT-induced cell killing.

## HNSCC Specimens Show Inverse Correlation between SMAD4 IHC Score and pH2AX accumulation

To assess if our preclinical findings are applicable to HNSCC patients, we examined pretreatment HNSCCs for their SMAD4 status and extent of DNA damage in specimens

collected in the phase I trial of olaparib in combination with RT and cetuximab, a standard of care for cisplatin ineligible, locally advanced HNSCC patients (17). Among 14 patients with available primary HNSCC specimens, 3 had HNSCC with *SMAD4* chromosomal loss as determined by the ratio of *SMAD4*/centromere 18 (CEN18) ratio (9) and showed no or little SMAD4 protein by IHC (Figure 6a). Three other patients had *SMAD4* wildtype HNSCCs with non-detectable levels of SMAD4 protein (Figure 6a), indicating post-genetic SMAD4 loss as previously reported (11). Five out of six of these patients showed no evidence of disease at time of death, and the one non-responder's tumor had a *KMT2A* mutation and *MYC* amplification associated with non-responsiveness (Figure 6a) (17). Among eight SMAD4 positive HNSCC cases, four showed no evidence of disease (Figure 6a). SMAD4 protein levels determined by IHC inversely correlated with the number of pH2AX+ cells (Figure 6b, 6c). Further, most pH2AX+ cells were Ki67 negative (Figure 6b) suggesting that cells with accumulated DNA damage could not enter cell cycle and proliferate.

## Discussion

### SMAD4 Levels Affect Therapeutic Response to Olaparib and RT Combination

Heterozygous *SMAD4* deletion occurs in 35–52% of HNSCCs (8,9). We have shown that heterozygous *SMAD4* deletion reduces *SMAD4* expression by 50% and confers haploid insufficiency (11). Our previous study using mouse HNSCCs and human HNSCC cell lines identified the causal role of SMAD4 loss in lowered expression of certain genes in the *FANC/BRCA* family (11), and our current study reveals this phenomenon in the large HNSCC TCGA dataset. Our finding, that a panel of *SMAD4* mutant HNSCC cell lines were sensitive to olaparib, suggests a predisposition for SMAD4 loss in therapeutic response of "BRCA-like" phenotypes. Beyond correlation, we found that *SMAD4* deficient HNSCCs were more responsive than *SMAD4*-positive HNSCCs to olaparib in combination with RT *in vivo*, in comparison with tumors derived from isogenic SMAD4-positive HNSCC cells. Although PARP inhibitors have efficacy as a monotherapy in *BRCA*-mutant ovarian cancer (28), not all *SMAD4* mutant HNSCC xenografts were eradicated by olaparib alone. Because tobacco-associated HNSCCs generally have a higher mutational load and a stronger survival ability than many other cancer types (4,29), HNSCC cells likely require a higher accumulation of DNA damage to induce DNA damage-associated cell death (30). To this end, in the presence of RT, olaparib increased RT-induced killing as seen in a previous *in vitro* study (31). In *SMAD4*-positive UMSCC1 HNSCC xenograft tumors, despite an initial yet temporary response to RT alone, xenograft tumors continued to grow in all therapeutic groups. However, when *SMAD4* was knocked down in UMSCC1 xenografts, dual treatment with olaparib and RT significantly reduced tumor size.

The differences in therapeutic response between HNSCCs with complete genetic *SMAD4* loss (CAL27) and *SMAD4* reduction (UMSCC1+*shSMAD4*) may represent a dose-dependent effect of *SMAD4* loss or other genetic alterations among different tumors. The complete abrogation of tumor growth by restoration of *SMAD4* in CAL27 cells suggests that tumorigenesis in CAL27 is largely driven by *SMAD4* loss. This *SMAD4* loss-dependent tumor development shows that *SMAD4* is a potent tumor suppressor even after cells have

transformed into HNSCC, consistent with a previous report (10). In contrast, UMSCC1 tumorigenesis does not rely on *SMAD4* loss as knocking down *SMAD4* did not affect tumor growth, but it did affect therapeutic response. While CAL27 do not harbor any loss-of-function *FANC/BRCA* mutations (based on the cancer cell line encyclopedia interrogation), and we cannot exclude the possibility that other genetic alternations in CAL27 tumors determines sensitivities to olaparib with/without RT, overall our data suggest that *SMAD4* loss may affect the therapeutic effects of olaparib with RT even in the presence of additional tumor drivers, as is the case with UMSCC1 cells (24).

### *SMAD4* Dose-Dependent Effects on DNA Damage and Associated Apoptosis in Response to PARP Inhibition with RT

*In vivo, SMAD4* deficient HNSCC xenografts incurred substantial apoptosis in response to all treatments compared to vehicle, consistent with their therapeutic response among all treatment groups. Except for apoptosis in UMSCC1+*shSMAD4* tumors, DNA damage and apoptosis in the olaparib + RT group were not significantly higher than each treatment alone at the end of tumor harvest time point. Therefore, reductions in *SMAD4* deficient HNSCC tumor volumes by dual olaparib + RT therapy are likely a consequence of early cell death as suggested by our *in vitro* studies.

In other tumor types, PARP inhibitors confer therapeutic effects via either blocking DNA repair or inducing formation of a PARP-DNA complex (“PARP-trapping”) to cause cytotoxic effects (32). If the latter mechanism occurs, a therapeutic effect is relatively rapid (33). In our study, *in vivo* olaparib treatment had a long latency before showing modest therapeutic benefit. Therefore, PARP inhibition appears to cause cell death primarily through disruption of DNA repair (30). It is possible that PARP inhibition alone causes single strand breaks (SSBs), but these are not sufficient to kill cells (30). However, as SSB-damaged cells divide and replicate they accumulate double strand breaks (DSBs), causing cell death later in treatment as we observed in xenograft tumor models. Because tobacco-associated HNSCC cells likely tolerate more extensive DNA damage compared to ovarian cells (3), HNSCCs require additional genotoxic insults, e.g. RT-induced damage, to reduce cell viability. Consistent with this notion, we found that olaparib combined with radiation was most effective in reducing clonogenic survival and inducing apoptosis in *SMAD4*-mutant HNSCC cells, and this effect was either weaker in *SMAD4*-positive HNSCC cells or attenuated by SMAD4 restoration in *SMAD4* mutant cells. Therefore, *SMAD4* likely plays a protective role in maintaining cell viability when exposed to genotoxic stress (11).

Consistent with decreased clonogenic survival by dual treatment with olaparib and radiation, DNA damage was more severe in *SMAD4* deficient cells compared to *SMAD4*-positive HNSCC cells or attenuated by SMAD4 restoration in *SMAD4* mutant cells *in vitro*. Although the clonogenic survival in response to olaparib with radiation was similar between UMSCC1+*shSMAD4* and CAL27 cells, radiation alone was more effective in CAL27 cells than in UMSCC1+*shSMAD4* cells. These findings suggest that complete genetic *SMAD4* loss has a more profound effect than *SMAD4* knockdown on therapeutic response targeting DNA repair. However, it is important to note that additional tumor drivers are also at play in both these cell lines.

### HNSCCs with SMAD4 Loss May Be Targetable by Olaparib and RT Combination Therapy

A previous report showed that olaparib sensitization of cancer cells to radiation depends on the integrity of homologous recombination defects (31). Therefore, HNSCCs may harbor homologous recombination defects independent of SMAD4 status and such HNSCCs may be equally sensitive to PARP inhibition (seen in two *SMAD4* wildtype HNSCC cell lines in Figure 1d, 1e). Our current and previous studies revealed that SMAD4 can also be lost at the post-genetic level. Further, SMAD4 loss in HNSCCs generally predicts a poor response to therapies (34), thus SMAD4 wildtype HNSCCs may represent a group of tumors that generally respond well to therapies. Taking these clinical complexities into consideration, our Phase I trial of olaparib with RT and cetuximab demonstrate patients responding to therapy with or without SMAD4 loss. Although the number of specimens is too small to draw any correlation, it is noted that 5/6 patients who have SMAD4 negative tumors demonstrated no evidence of disease compared to 4/8 SMAD4 positive patients and the one progressed SMAD4 negative tumor harbors *KMT2A* mutation and *MYC* amplification, molecular alterations suggested for a non-responding correlation (17). Because the baseline SMAD4 protein level inversely correlated with the extent of accumulated DNA damage in these patient specimens, future studies with larger patient numbers should assess whether the combination of SMAD4 status and/or the extent of DNA damage can be used to correlate the therapeutic response to PARP inhibition in combination with RT.

In summary, our preclinical study provides evidence that *SMAD4* loss contributes to the therapeutic response of olaparib combined with RT. Our findings provide insight into the design of a biomarker-driven therapeutic intervention using olaparib in combination with RT to treat HNSCC patients that will potentially improve clinical outcomes. Future studies will further delineate molecular mechanisms of RT and PARP inhibitor therapy with respect to SMAD4 status, and identify which *FANC/BRCA* family genes are direct transcriptional targets of SMAD4; hence their downregulation or baseline pH2AX may serve as alternative predictive markers for therapeutic response to DNA damaging agents in HNSCCs.

## Supplementary Material

Refer to Web version on PubMed Central for supplementary material.

## Acknowledgements

This work was supported by NIH grant DE015953 and VA Merit Award 1 I01 BX003232 to XJW. ALH was supported by T32 CA174648. KW was supported by T32 CA174648 and F32DE027285. DR, SDK and ALH were supported by the Marsico Endowment and an anonymous donation for HNSCC research. We thank Astra Zeneca for providing olaparib for *in vivo* studies, Nicole Manning and Lisa DePledge for technical assistance. Dr. Thomas Carey for advice and an anonymous donation for support of this work. Pamela Garl provided critical proof reading of this manuscript.

## References

1. Bertsch NS, Bindler RJ, Wilson PL, Kim AP, Ward B. Medication Therapy Management for Patients Receiving Oral Chemotherapy Agents at a Community Oncology Center: A Pilot Study. Hosp Pharm 2016;51:721–9 [PubMed: 27803501]

2. Mendenhall WM, Mancuso AA, Amdur RJ, Stringer SP, Villaret DB, Cassisi NJ. Squamous cell carcinoma metastatic to the neck from an unknown head and neck primary site. Am J Otolaryngol 2001;22:261–7 [PubMed: 11464323]

3. Ang KK, Harris J, Wheeler R, Weber R, Rosenthal DI, Nguyen-Tan PF, et al. Human papillomavirus and survival of patients with oropharyngeal cancer. N Engl J Med 2010;363:24–35 [PubMed: 20530316]

4. Leemans CR, Braakhuis BJ, Brakenhoff RH. The molecular biology of head and neck cancer. Nat Rev Cancer 2011;11:9–22 [PubMed: 21160525]

5. Moeller BJ, Yordy JS, Williams MD, Giri U, Raju U, Molkentine DP, et al. DNA repair biomarker profiling of head and neck cancer: Ku80 expression predicts locoregional failure and death following radiotherapy. Clin Cancer Res 2011;17:2035–43 [PubMed: 21349997]

6. Kutler DI, Auerbach AD, Satagopan J, Giampietro PF, Batish SD, Huvos AG, et al. High incidence of head and neck squamous cell carcinoma in patients with Fanconi anemia. Arch Otolaryngol Head Neck Surg 2003;129:106–12 [PubMed: 12525204]

7. Feldman R, Gatalica Z, Knezetic J, Reddy S, Nathan CA, Javadi N, et al. Molecular profiling of head and neck squamous cell carcinoma. Head Neck 2016;38 Suppl 1:E1625–38 [PubMed: 26614708]

8. Snijders AM, Schmidt BL, Fridlyand J, Dekker N, Pinkel D, Jordan RC, et al. Rare amplicons implicate frequent deregulation of cell fate specification pathways in oral squamous cell carcinoma. Oncogene 2005;24:4232–42 [PubMed: 15824737]

9. Hernandez AL, Wang Y, Somerset HL, Keysar SB, Aisner DL, Marshall C, et al. Inter- and intra-tumor heterogeneity of SMAD4 loss in head and neck squamous cell carcinomas. Mol Carcinog 2019;58:666–73 [PubMed: 30575147]

10. Reiss M, Santoro V, de Jonge RR, Vellucci VF. Transfer of chromosome 18 into human head and neck squamous carcinoma cells: evidence for tumor suppression by Smad4/DPC4. Cell Growth Differ 1997;8:407–15 [PubMed: 9101086]

11. Bornstein S, White R, Malkoski S, Oka M, Han G, Cleaver T, et al. Smad4 loss in mice causes spontaneous head and neck cancer with increased genomic instability and inflammation. J Clin Invest 2009;119:3408–19 [PubMed: 19841536]

12. Lee JM, Ledermann JA, Kohn EC. PARP Inhibitors for BRCA1/2 mutation-associated and BRCA-like malignancies. Annals of oncology : official journal of the European Society for Medical Oncology / ESMO 2014;25:32–40

13. Stoppa-Lyonnet D The biological effects and clinical implications of BRCA mutations: where do we go from here? Eur J Hum Genet 2016;24 Suppl 1:S3–9 [PubMed: 27514841]

14. Nijman SM. Synthetic lethality: general principles, utility and detection using genetic screens in human cells. FEBS letters 2011;585:1–6 [PubMed: 21094158]

15. Dedes KJ, Wilkerson PM, Wetterskog D, Weigelt B, Ashworth A, Reis-Filho JS. Synthetic lethality of PARP inhibition in cancers lackingBRCA1andBRCA2mutations. Cell Cycle 2014;10:1192–9

16. Somyajit K, Mishra A, Jameei A, Nagaraju G. Enhanced non-homologous end joining contributes toward synthetic lethality of pathological RAD51C mutants with poly (ADP-ribose) polymerase. Carcinogenesis 2015;36:13–24 [PubMed: 25292178]

17. Karam SD, Reddy K, Blatchford PJ, Waxweiler T, DeLouize AM, Oweida A, et al. Final Report of a Phase I Trial of Olaparib with Cetuximab and Radiation for Heavy Smoker Patients with Locally Advanced Head and Neck Cancer. Clin Cancer Res 2018;24:4949–59 [PubMed: 30084837]

18. Gao J, Aksoy BA, Dogrusoz U, Dresdner G, Gross B, Sumer SO, et al. Integrative analysis of complex cancer genomics and clinical profiles using the cBioPortal. Sci Signal 2013;6:pl 1

19. Cerami E, Gao J, Dogrusoz U, Gross BE, Sumer SO, Aksoy BA, et al. The cBio cancer genomics portal: an open platform for exploring multidimensional cancer genomics data. Cancer Discov 2012;2:401–4 [PubMed: 22588877]

20. Han G, Bian L, Li F, Cotrim A, Wang D, Lu J, et al. Preventive and therapeutic effects of Smad7 on radiation-induced oral mucositis. Nature medicine 2013;19:421–8

21. Fowler JF. The linear-quadratic formula and progress in fractionated radiotherapy. Br J Radiol 1989;62:679–94 [PubMed: 2670032]

22. Gioanni J, Fischel JL, Lambert JC, Demard F, Mazeau C, Zanghellini E, et al. Two new human tumor cell lines derived from squamous cell carcinomas of the tongue: establishment, characterization and response to cytotoxic treatment. Eur J Cancer Clin Oncol 1988;24:1445–55 [PubMed: 3181269]

23. David CJ, Huang YH, Chen M, Su J, Zou Y, Bardeesy N, et al. TGF-beta Tumor Suppression through a Lethal EMT. Cell 2016;164:1015–30 [PubMed: 26898331]

24. Brenner JC, Graham MP, Kumar B, Saunders LM, Kupfer R, Lyons RH, et al. Genotyping of 73 UM-SCC head and neck squamous cell carcinoma cell lines. Head Neck 2010;32:417–26 [PubMed: 19760794]

25. Murai J, Huang SY, Renaud A, Zhang Y, Ji J, Takeda S, et al. Stereospecific PARP trapping by BMN 673 and comparison with olaparib and rucaparib. Mol Cancer Ther 2014;13:433–43 [PubMed: 24356813]

26. Jdey W, Thierry S, Russo C, Devun F, Al Abo M, Noguiez-Hellin P, et al. Drug-Driven Synthetic Lethality: Bypassing Tumor Cell Genetics with a Combination of AsiDNA and PARP Inhibitors. Clin Cancer Res 2017;23:1001–11 [PubMed: 27559053]

27. Polak P, Kim J, Braunstein LZ, Karlic R, Haradhavala NJ, Tiao G, et al. A mutational signature reveals alterations underlying deficient homologous recombination repair in breast cancer. Nat Genet 2017;49:1476–86 [PubMed: 28825726]

28. Lorusso D, Tripodi E, Maltese G, Lepori S, Sabatucci I, Bogani G, et al. Spotlight on olaparib in the treatment of BRCA-mutated ovarian cancer: design, development and place in therapy. Drug Des Devel Ther 2018;12:1501–9

29. Alexandrov LB, Ju YS, Haase K, Van Loo P, Martincorena I, Nik-Zainal S, et al. Mutational signatures associated with tobacco smoking in human cancer. Science 2016;354:618–22 [PubMed: 27811275]

30. Dziadkowiec KN, Gasiorowska E, Nowak-Markwitz E, Jankowska A. PARP inhibitors: review of mechanisms of action and BRCA1/2 mutation targeting. Prz Menopauzalny 2016;15:215–9 [PubMed: 28250726]

31. Verhagen CV, de Haan R, Hageman F, Oostendorp TP, Carli AL, O'Connor MJ, et al. Extent of radiosensitization by the PARP inhibitor olaparib depends on its dose, the radiation dose and the integrity of the homologous recombination pathway of tumor cells. Radiother Oncol 2015;116:358–65 [PubMed: 25981132]

32. Pommier Y, O'Connor MJ, de Bono J. Laying a trap to kill cancer cells: PARP inhibitors and their mechanisms of action. Sci Transl Med 2016;8:362ps17

33. Murai J, Huang SY, Das BB, Renaud A, Zhang Y, Doroshow JH, et al. Trapping of PARP1 and PARP2 by Clinical PARP Inhibitors. Cancer Res 2012;72:5588–99 [PubMed: 23118055]

34. Ozawa H, Ranaweera RS, Izumchenko E, Makarev E, Zhavoronkov A, Fertig EJ, et al. SMAD4 Loss Is Associated with Cetuximab Resistance and Induction of MAPK/JNK Activation in Head and Neck Cancer Cells. Clin Cancer Res 2017;23:5162–75 [PubMed: 28522603]

## Translational Relevance

Despite advances in therapeutic approaches, survival rates remain poor for head and neck squamous cell carcinoma (HNSCC) patients. SMAD4 deficient HNSCCs present a "BRCA-like" phenotype, and our current study also revealed "BRCA-like" molecular signatures, i.e., reduced expression of the FANC (Fanconi Anemia Complementation)/ BRCA (breast cancer susceptibility) family genes in human HNSCC specimens with SMAD4 loss. Our study provides evidence that SMAD4 loss sensitizes HNSCCs to therapeutic response to a PARP inhibitor that targets the "BRCA-like" phenotype in combination with radiotherapy (RT), a standard therapy for locally advanced HNSCCs. Our findings provide important insight into designing future biomarker-based clinical trials to test whether *SMAD4* deficient HNSCCs can be effectively treated with this therapeutic intervention.

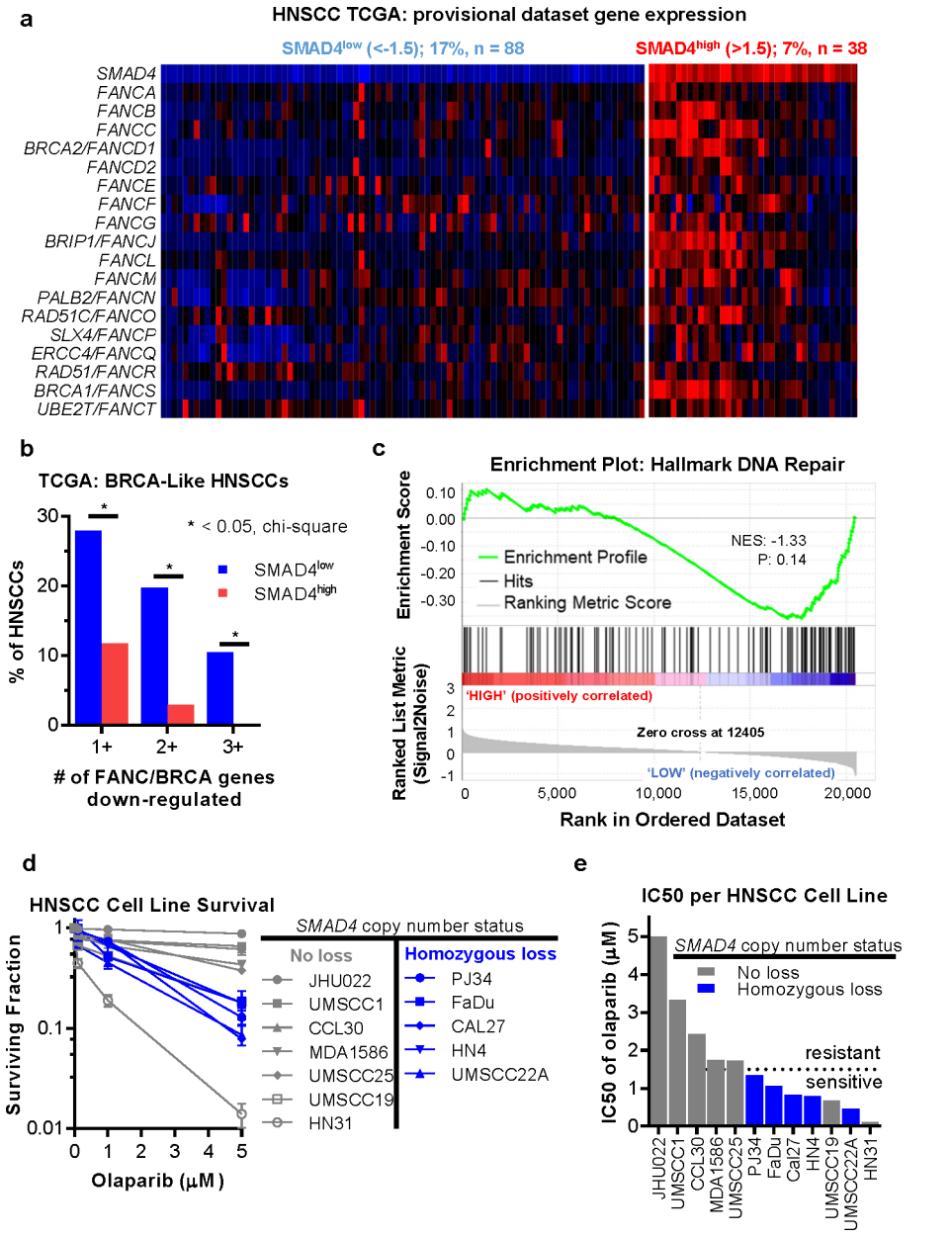


**Figure 1. Low *SMAD4* expression correlates with low *FANC/BRCA* gene expression in HNSCC patient specimens and olaparib sensitivity.**

(a) Analysis of human HNSCCs gene expression organized by z-score to compare *SMAD4* mRNA expression with *FANC/BRCA* family gene expression in the provisional TCGA cohort including 530 cases downloaded from cbioportal. This analysis included the 88 patients with *SMAD4* expression 1.5 standard deviations below the mean (SMAD4$^{low}$) and 38 patients with *SMAD4* expression 1.5 standard deviations above the mean (SMAD4$^{high}$). (b) The number of *FANC/BRCA* family genes down-regulated (1.5 standard deviations below the mean) related to *SMAD4* levels in patients' HNSCCs was evaluated by Chi-square analysis (*: $p<0.05$). (c) Gene expression profiles of SMAD4$^{high}$ and SMAD4$^{low}$ patients was analyzed by GSEA against the 50 hallmark gene sets downloaded from

MSigDB (Broad Institute). Enrichment plot, Normalized enrichment score (NES) and p value for the “DNA repair” hallmark gene set is presented. (d) The olaparib surviving fraction and (e) olaparib IC50 for the indicated cell lines (with no *SMAD4* deletion or homozygous *SMAD4* loss) was determined by clonogenic assay (6 technical replicates).

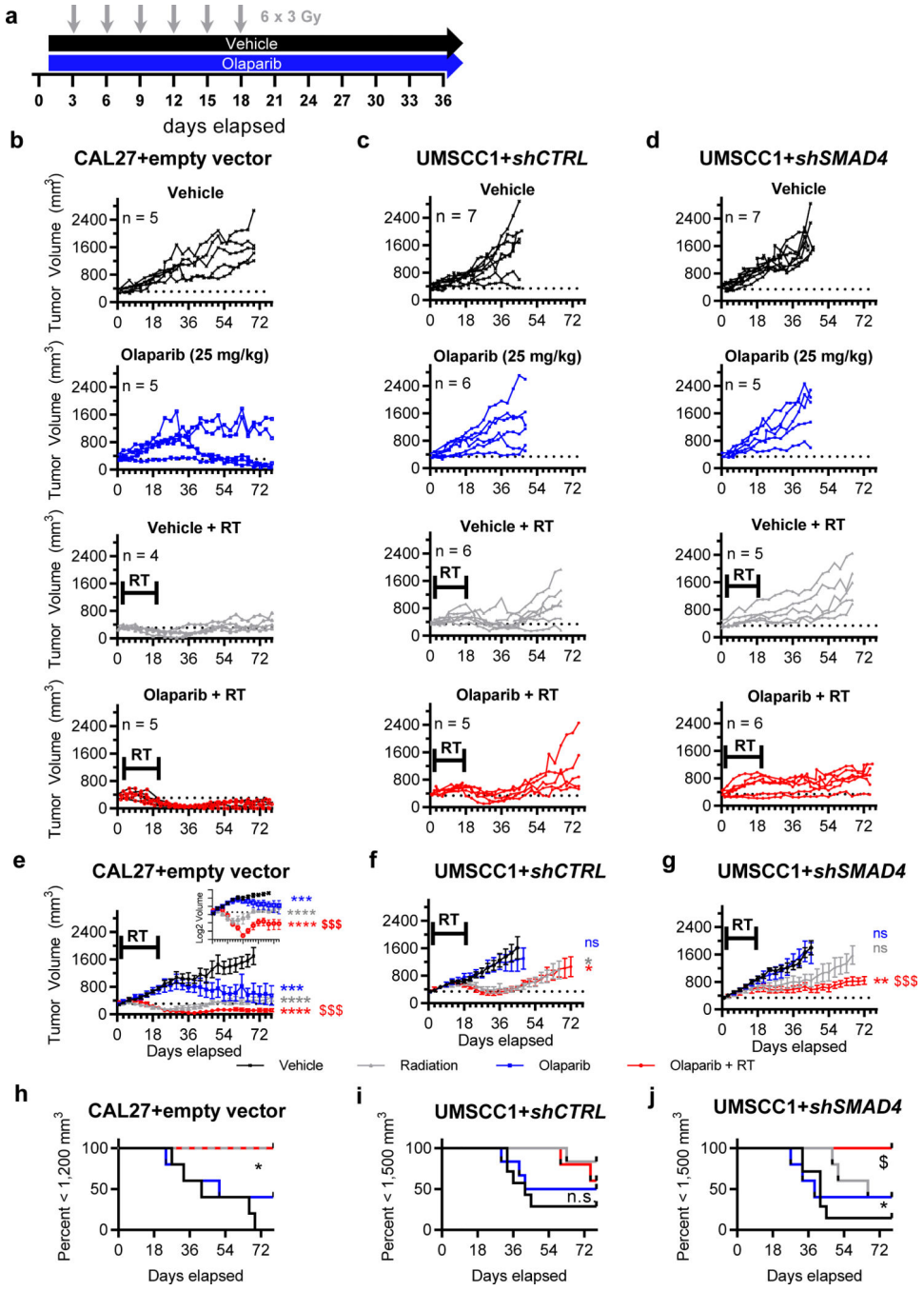


**Figure 2. The combination of olaparib and RT uniquely inhibits the growth of *SMAD4*-deficient HNSCCs *in vivo*.**

(a) Mice were transplanted with tumors cells and when tumors reached 300 $mm^3$, mice were randomized into treatment groups, receiving daily olaparib (25 mg/kg) or vehicle treatments beginning on day 1 and continuing for the duration of the study and/or six 3 Gy doses of RT every three days as indicated in the schematic. (b-d) The size of individual CAL27+empty vector (b), UMSCC1+*shCTRL* (c), and UMSCC1+*shSMAD4* (d) tumors undergoing each treatment is plotted against time. (e-g) Average tumor size (+/− SEM) in each treatment group in the indicated tumor types is plotted and analyzed by mixed-effects model with

Tukey's multiple comparison test comparing vehicle to each treatment group *: p<0.05; **: p<0.01; ***: p<0.001; ****: p<0.0001 or RT vs dual treatment $ $ $: p<0.001. The inset plots CAL27 tumor volume data on a log2 scale to better differentiate between small tumors. (h - j). The number of tumors < 1,200 $mm^3$ (CAL27) or < 1,500 $mm^3$ (UMSCC1) is plotted over time and analyzed by log rank test (*: $p < 0.05$; comparing all four treatment groups; $: $p < 0.05$ comparing dual treatment to RT alone).

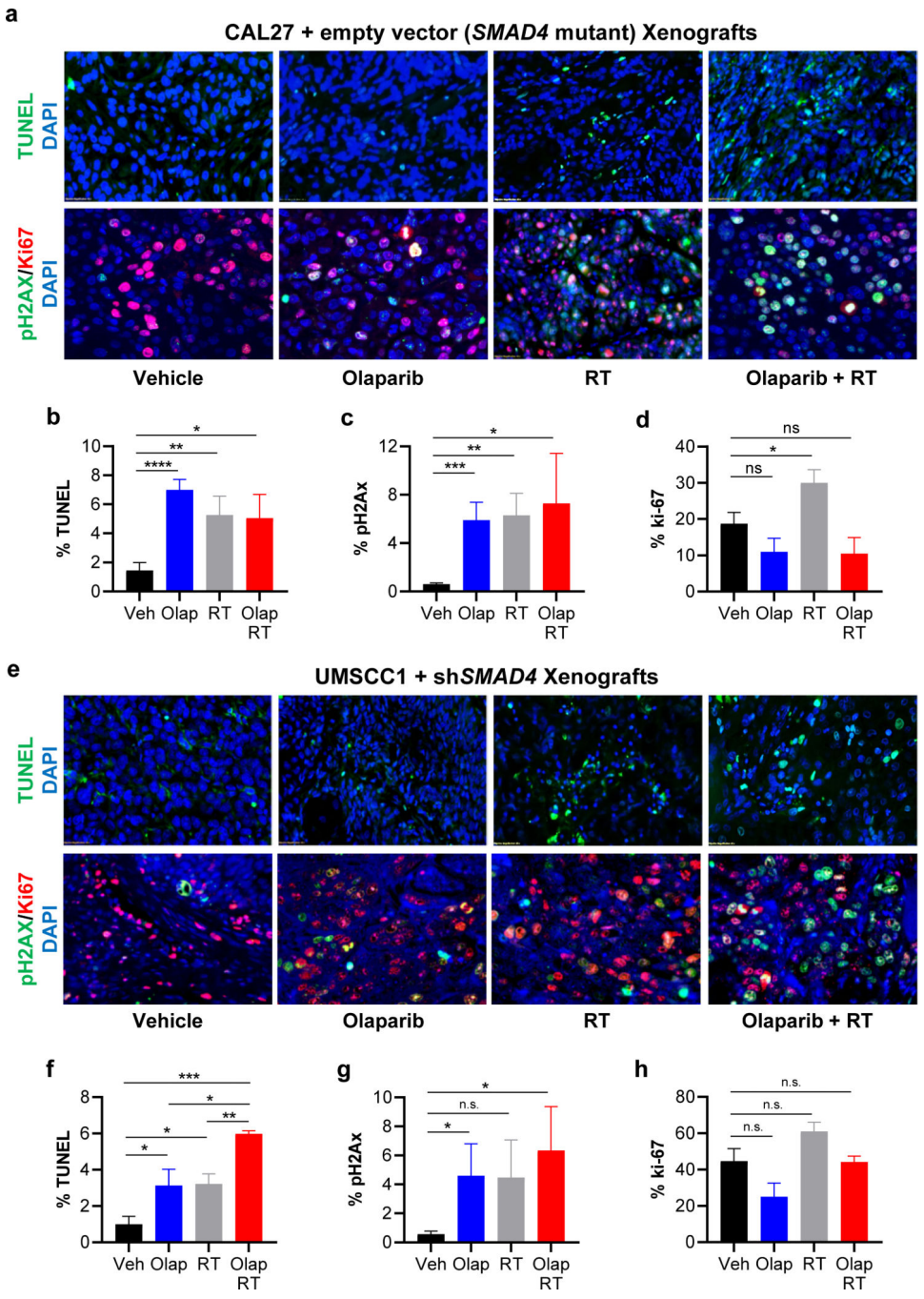


**Figure 3. Increased DNA damage and apoptosis in *SMAD4* deficient HNSCCs with treatments *in vivo*.**

Representative images of TUNEL (green, top), pH2AX (green, bottom), and Ki67 (red, bottom) staining in CAL27+empty vector tumors (a) at 40x magnification. Percentage of positive cells for TUNEL (b), pH2AX (c), and Ki67 (d) were quantified using 3 – 7 tumor samples per group. Representative images of TUNEL, pH2AX, and Ki67 staining in UMSCC1+*shSMAD4* tumors (e) at 40x magnification. Percentage of positive cells for TUNEL (f), pH2AX (g), and Ki67 (h) was quantified per tumor, presented as mean +/−SEM. DAPI counterstain for all tumors. Quantification of each treatment was analyzed vs

vehicle or dual treatment vs single treatment by Student's t-test, *: $p < 0.05$; **: $p < 0.01$; ***: $p < 0.001$; ****: $p < 0.0001$.

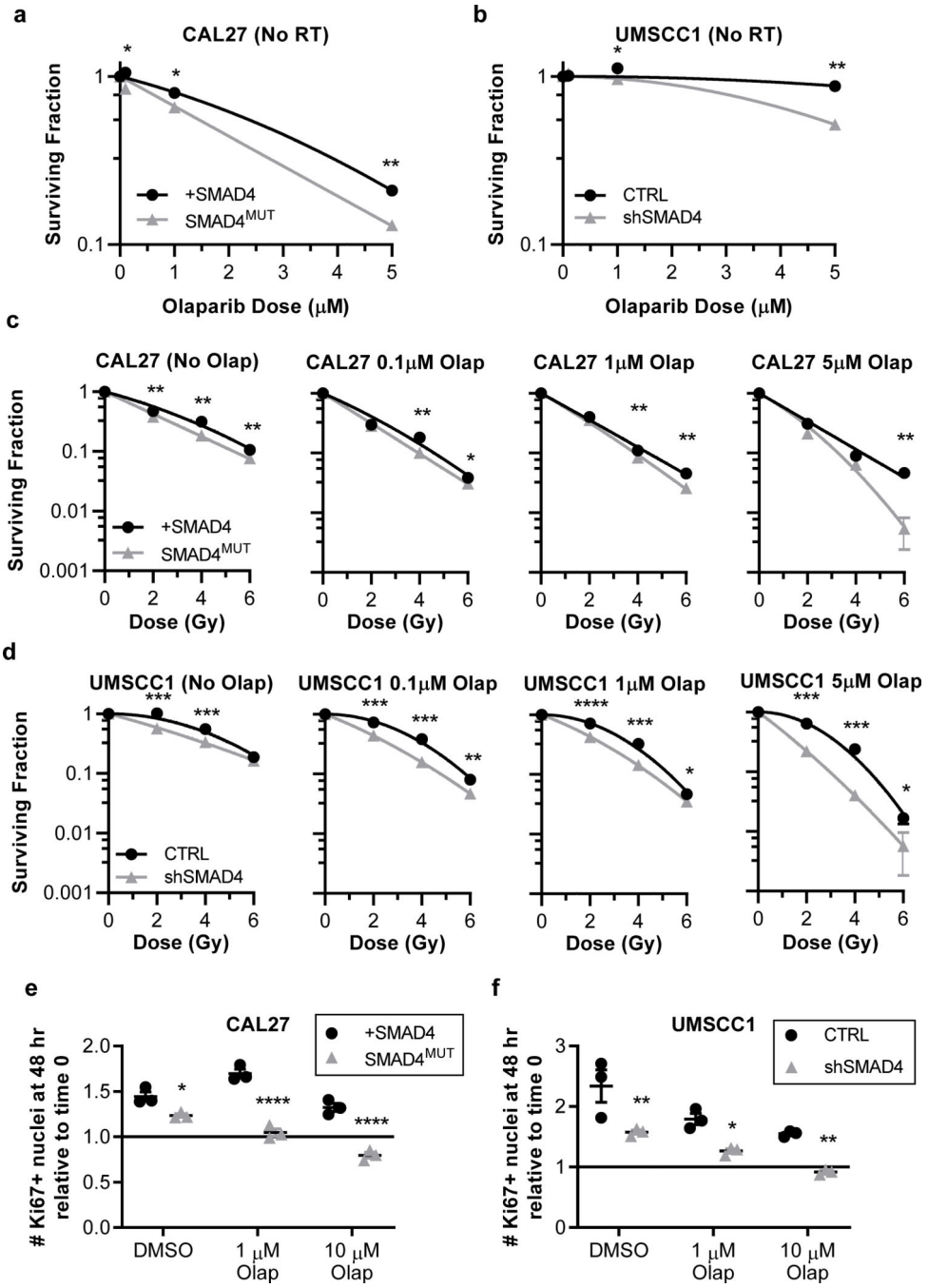


**Figure 4. Olaparib and radiation decrease clonogenic outgrowth and proliferation more potently in *SMAD4*-deficient HNSCC cells *in vitro*.**

(a-d) CAL27+dox-inducible *SMAD4* and UMSCC1+dox-inducible *SMAD4* shRNA treated +/− doxycycline to induce respective gene expression were seeded to twelve well plates. 18 hr later, plates were exposed to 0–5 μM olaparib (Olap) that was maintained for the duration of the assay and a single dose of 0–6 Gy RT. Plates were fed fresh media with/without doxycycline and olaparib every three days until colony formation was established and stained with crystal violet. The surviving fraction of colonies was determined by clonogenic assay and analyzed by Student's t-test comparing $SMAD4^{+}$ to $SMAD4^{-/low}$ groups *: p <

0.05; **: p < 0.01; ***: p < 0.001; ****: p < 0.0001. (e, f) Ki67 staining was quantified prior to (0 hour) and 48 hours after 8 Gy RT in DMSO and olaparib treated cells, analyzed by Student's t-test comparing *SMAD4*$^{+}$ to *SMAD4*$^{-/low}$ groups *: p<0.05; **: p<0.01; ****: p<0.0001. Each experiment was performed with two independent repeats and one representative experiment is presented (mean +/−SEM).

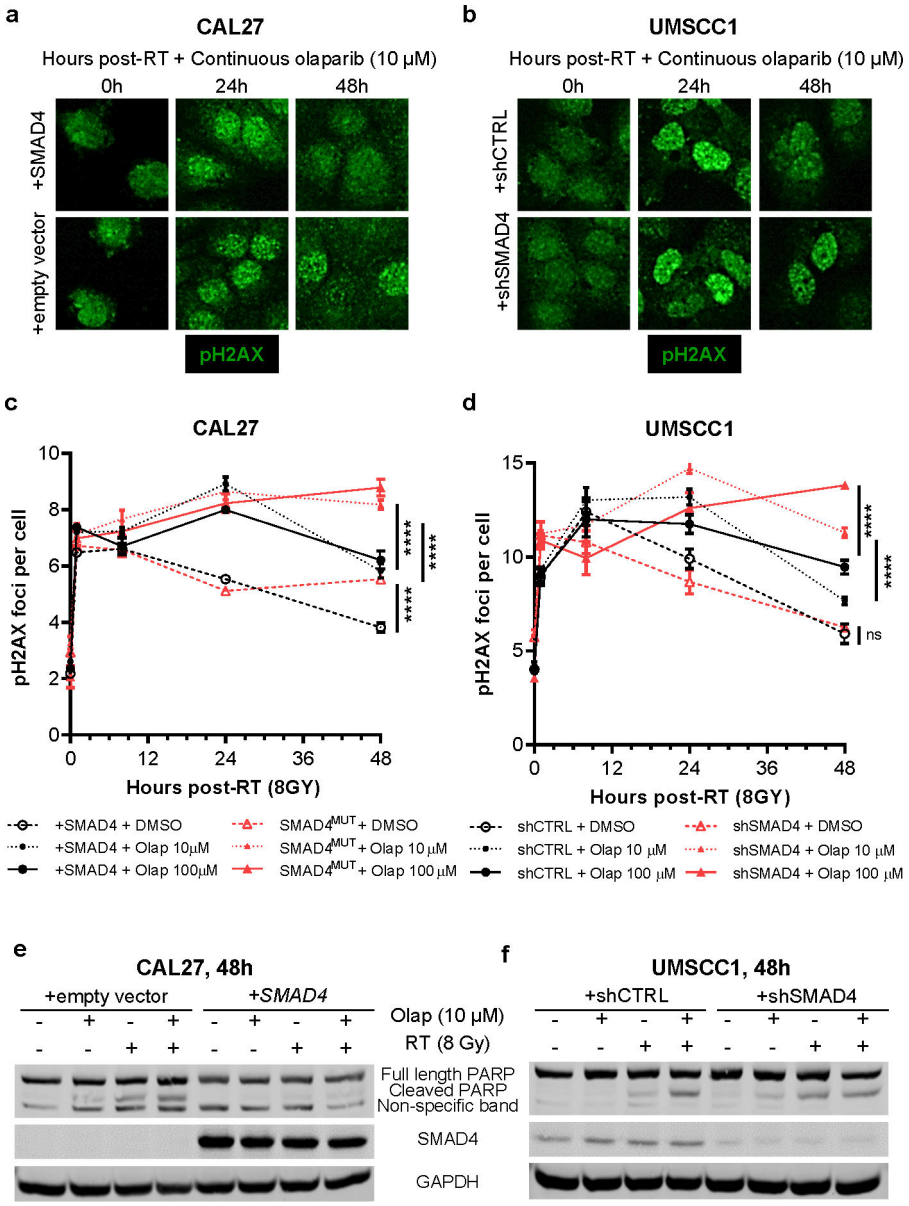


**Figure 5. Olaparib and radiation increase DNA damage and associated apoptosis more potently in SMAD4-deficient HNSCC cells *in vitro*.**

Representative pH2AX images of CAL27 (a) and UMSCC1 (b) isogenic cells at 0, 24 and 48-hours post- treatment with 8 Gy radiation and continuous 10 μM olaparib. (c-d) Quantification of pH2AX foci at all time points and treatment groups was analyzed by two-way ANOVA with Sidak's multiple comparison test comparing *SMAD4*$^{+}$ to *SMAD4*$^{-/low}$ groups ****: $p > 0.0001$ (6 replicates). All plots represent mean +/− SEM. Two independent repeats were performed and one representative experiment is presented (mean +/−SEM). (e-f) Western blot for PARP, cleaved PARP, SMAD4 and GAPDH, in CAL27+/−*SMAD4* (e) and UMSCC1+/−*SMAD4* (f) lysates harvested 48 hr after the indicated treatments.

a

| Study ID* | PFS† (months)/Presence of disease | *KMT2A* mutant | *MYC* amplified | SMAD4/ CEN18‡ | SMAD4 IHC score# | pH2AX score¥ |
|---|---|---|---|---|---|---|
| 1 | 48 /NED§ | No | No | 0.95 | 0.5 (loss) | 3 |
| 2 | 6/NED | No | No | 0.41 (loss) | 0 (loss) | 3 |
| 3 | 31/progress to second cancer | No | No | 0.93 | 1 | 3 |
| 4 | 45/NED | No | No | 0.98 | 3 | 1 |
| 5 | 20/NED | No | No | 1 | 2 | 1 |
| 6 | 39/NED | | | 0.95 | 2.5 | 1 |
| 7 | 8/metastasis | Yes | Yes | 0.26 (loss) | 0.5 (loss) | 3 |
| 9 | 38/NED | | | 0.5 (loss) | 0 (loss) | 3 |
| 10 | 24/NED | | | 1 | 0 (loss) | 3 |
| 11 | NED, withdrew 4 cetuximab cycle/ 24RT fractions | | | 1 | 0 (loss) | 3 |
| 12 | 11/local recurrent | | | 1.1 | 1 | 1 |
| 14 | 9/NED | No | No | 0.84 | 2 | 2 |
| 15 | 8/metastasis | Yes | Yes | 0.96 | 1 | 3 |
| 16 | 8/local recurrent | No | Yes | 0.65 | 1.5 | 1 |

*: Phase I trial of olaparib plus RT and cetuximab (Karam et al., CCR, DOI: 10.1158/1078-0432, 2018)
†: Progression-free survival
‡: SMAD4 chromosomal loss determined by fluorescence in situ hybridizationSMAD4/Centromere 18 (CEN18) < 0.5 (Hernandez, et al., Mol. Carcinog., 2019)
#: 0: background staining similar to CAL27 HNSCC; 1: or 2: uniform (1) or < 30% area reduction compared to normal mucosa, 3: equivalent to normal mucosa
¥: 1: < 20% of foci-positive cells, 2: 20% - < 50% positive cells, 3: >50% positive cells
§: no evidence of disease

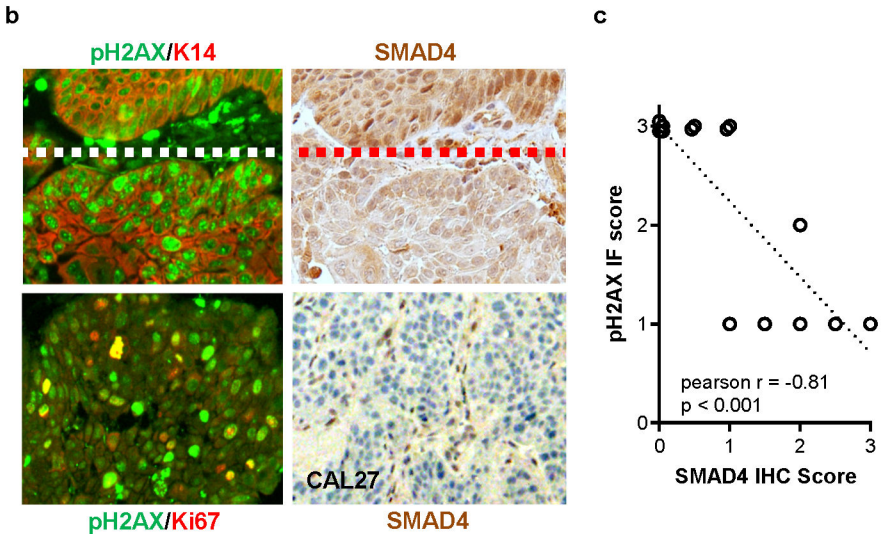


**Figure 6. SMAD4 and pH2AX status in primary HNSCCs and clinical outcomes in the olaparib + RT + cetuximab trial.**

(a) Table describing the progression free survival (PFS), presence of disease, *KMT2A* mutation, *MYC* amplification, SMAD4/CEN18 ratio (determined by FISH), and IHC scores for SMAD4 and pH2AX in the 14 patients evaluated in the trial. (b) Representative immunostaining images of SMAD4, pH2AX, and Ki67. Dotted lines in upper panels highlight consecutive sections of pH2AX+ low vs. high sections inversely mirrored with $SMAD4^{high}$ vs. $SMAD4^{low}$ staining. Lower left panel presents the same tumor, stained for pH2AX and Ki67 which are largely mutually exclusive. Lower right panel presents SMAD4 IHC optimized using CAL27 xenograft tumor in which mouse Smad4 positive cells are in

tumor stroma but not in tumor epithelia (human SMAD4). (c) Inverse correlation between SMAD4 IHC scores and pH2AX scores from specimens listed in panel a.